UNIVERSITY OF CALIFORNIA, SAN DIEGO

Porous Iron Structure Fabrication and Characterization

A Thesis submitted in partial satisfaction of the

requirements for the degree Master of Science

in

Materials Science and Engineering

by

Taewoo Kim

Committee in Charge:

Professor Sungho Jin, Chair
Professor Rencun Chen
Professor Zhaowei Liu

2015

The Thesis of Taewoo Kim is approved, and it is acceptable in quality and form for publication on microfilm:

Chair

University of California, San Diego

2015

DEDICATION

Dedicated to

my family

EPIGRAPH

"There are two ways to live: you can live as if nothing is a miracle; you can live as if everything is a miracle."

Albert Einstein

TABLE OF CONTENTS

LIST OF FIGURES

LIST OF TABLES

ACKNOWLEDGEMENTS

First and foremost, I wish to acknowledge and deeply thank my advisor, Professor Sungho Jin for his steadfast encouragement, guidance, and support during the course of this research here at University of California, San Diego. I sincerely thank to my dissertation committee members for their precious time and helpful suggestions: Professor Rencun Chen, Professor Zhaowei Liu.

I wish to express my gratefulness to the JIN Group members for their numerous help, stimulating discussions, and invaluable contributions. I appreciate all the helps from my collaborators. In retrospect, it was a hardship, hence pleasure, to face numerous tangled problems and unravel a complicated problem one by one. Priceless memories shared with each of you will be in my heart for the rest of my life.

I would like to thank Korean seniors and juniors in UC, San Diego and their family for helping me in the aspects of not only various academic matters but also everyday life in San Diego. It was my great pleasure to share memories with each of you.

Finally, I wish to thank my dear family members for their cares, supports, and sacrifices shown not only through the course of this time but also the moment I am not recognized. Last but not least, I wish to express my infinite gratitude to my beloved wife, Miyoung Jeong and my lovely daughters, Gayul and Seoyul for sharing all sorts of emotions.

ABSTRACT OF THE THESIS

Porous Iron Structure Fabrication and Characterization

by

Taewoo Km

Master of Science in Materials Science and Engineering

University of California, San Diego, 2015

Professor Sungho Jin, Chair

Porous iron or steel structures can be useful as light-weight materials for transportation and structural applications. We have created such porous iron metallic structures by utilizing a composite of Fe2O3 nanoparticles (NPs), poly (methyl methacrylate) (PMMA) beads and polyethylene glycol (PEG) binder resin. Final optimized porous iron structure contains micro-pores of 15-20 μm size and nano-pores of 100-500 nm with strong connections between Fe grains. The results indicate that further efforts to develop advanced lightweight and strong materials may warrant potential applications such as bulletproof materials for helmets, light-weight vehicles, and for porous rocket engine.

CHAPTER 1: Introduction

Porous metal structures have attracted significant interest in recent years because of their potential applications in light-weight energy saving vehicles, porous rocket engines, and gas storage and separation devices.[1,2] Porous materials research has progressed and attracted tremendous attention, as can be seen from the rapidly increasing number of publications devoted to this field.[3] Although porous metal structures have many advantages, it would be helpful to increase the tensile strength and lightness of the materials by using nano-scale grains which makes tougher structure.[4] There are many techniques for fabrication of porous metal structures including combustion synthesis and replication. In case of the combustion synthesis method, a very fast self-sustaining exothermic reaction is carried out by the large amount of heat released in the synthesis.[5] First, the reactants are dried, mixed and cold–pressed. An exothermic reaction is then used to generate the heat and consolidate/fabricate the porous structure. In the case of replication, adaptive foam is used to make a porous structure.[6] The first step in one of the example replication processes is to make a slurry using a metal-based powder such as titanium hydride. The slurry is then coated several times onto polyurethane templates. After infiltration and complete drying, pattern removal is carried out.[7]

In the current study, three steps were taken to make the porous metal structure: (i) creating/mixing the slurry, (ii) coating the slurry on template, and (iii) heat treatment (burning and reduction) of the coated layer made of metal oxide, PMMA beads, and PEG binder resin. The focus was on optimizing conditions to obtain an ideal porous metal structure. To adjust the pore distribution and strong network connection of the

porous metal structure, several approaches were used. Three important variables were considered to create the desired structure : (i) the ratio of Fe2O3 nanoparticles (NPs) to PMMA beads, (ii) the ratio of Fe2O3 NPs to PEG binder, and (iii) the temperature of burning and reduction. The conditions were evaluated and optimized.

There are significant advantages to our method of making porous metal structures as compared to previous methods. First, our method uses a scalable fabrication technique for making the porous metal. The resultant porous iron structure consists of nano-scale grains which have many favorable properties including much higher tensile strength due to the Hall-Petch relationship.[8,9] Also, our porous structures were made without the use of additional foam utilized in previous research. Pore size was well controlled with the selection of PMMA beads size. The space left by the burned-away PMMA beads formed the well distributed pore structures, and the desirable nano-scale grains were made by sintering during the process of reduction heat treatment. Porous structures have a significant ability to absorb impact generated by collision.[10] A raw material for making the porous metal structure, Fe2O3 NPs, is abundant and inexpensive.[11] Fe particles are strong enough to obtain higher tensile strength especially made into nanograined structure.[12] Mass production can also be facilitated using solution coating, drying, and heat-treatment. Porous metal structures are important for developing lighter and stronger materials which are critical to improving protective equipment such as military helmets or bulletproof vest, to make alternative energy-saving, light weight vehicles more energy efficient and cost-effective, and to produce porous rocket engines.[13,14] New porous metal structures having desirable physical and metallurgical properties are needed in order to make more powerful equipment in the industry as well as military fields.[15]

CHAPTER 2: Porous Iron Structure Fabrication and Characterization

2.1 Methods

2.1.1 Fabrication of porous metal structures

The solubility experiment was carried out with polyethylene glycol (PEG) in some solvents. The optimized PEG solution consisted of 70 wt% PEG dissolved in a co-solvent of EtOH and H_2O (EtOH / H_2O = 7 / 3 [v/v]). In order to uniformly mix the composite solution consisting of Fe_2O_3 NPs (Alfa Aesar, average diameter=30nm), PMMA beads (cospheric, average diameter=50um) and PEG binder resin (Alfa Aesar), ball-mixing in an attrition mill was used with zirconia balls. The mixing process was performed for 48h at 120 rpm (21 s^{-1}). Coating process was performed on a Ni-plate substrate cleaned in acetone. After Doctor blade coating, the sample was dried at 35°C for 24h to remove the solvent from the coated layer. A burning process (heating rate: 5°C/min) in air atmosphere was carried out at two different conditions of 950°C for 2h and 1,050°C for 2h to make porous structure by removing PMMA beads from the composite layer. After the burning process, a reduction step was carried out in order to transform iron oxide to metallic iron and form the porous structure by heat treatment at different conditions of 500°C for 5h and 750°C for 5h in forming gas (5% H_2/95% N_2).

2.1.2 XRD and SEM analysis

X-ray diffraction (XRD) analysis was carried out to investigate the crystal structure of the reduced porous iron structure. The reduction heat treatment, once a sufficiently long time is given, transforms iron oxide in porous structure into pure iron. The burned composite layer was treated with reduction heat treatment followed by the analysis with XRD (Bruker D2 Phase XRD machine with CuK_α (λ=0.154 nm) as the radiation source). The scanning of 2θ angle was made in the range of 15^o-80^o with a

scanning rate of 1.5 deg./min. Scanning electron microscope (SEM) (Oxford) images were taken with an acceleration energy of 10KeV to observe the porous iron structure.

2.1.3 Thermogravimetry analysis (TGA)

Through TGA, the appropriate temperature could be found for the decomposition of composite materials. The sample was placed in an alumina pan and heated from 25°C to 1,500°C with a heating rate of 25°C / min in air ambient.

2.2 Results and discussion

The analysis on properties of the materials is important in order to optimize fabrication conditions which can make much lighter and stronger porous metal structures. TGA was used to determine the decomposition temperature for the porous metal structure. Figure 1 shows the decomposition temperature of the coated composite layer. PMMA beads and PEG binder resin are decomposed completely during heating to above 400°C under air atmosphere. Two step decomposition behavior is seen in the TGA analysis. The first step is to remove solvents of EtOH and H_2O up to 150°C. The second step is to decompose PMMA beads and PEG binder up to 400°C. Based on the decomposition temperature seen by TGA, the burning process of PMMA beads and PEG binder is selected to be at two different conditions 950°C and 1,050°C. When the burning process is applied to the composite layer, the PMMA beads and PEG binder were eliminated but the Fe_2O_3 NPs remained.

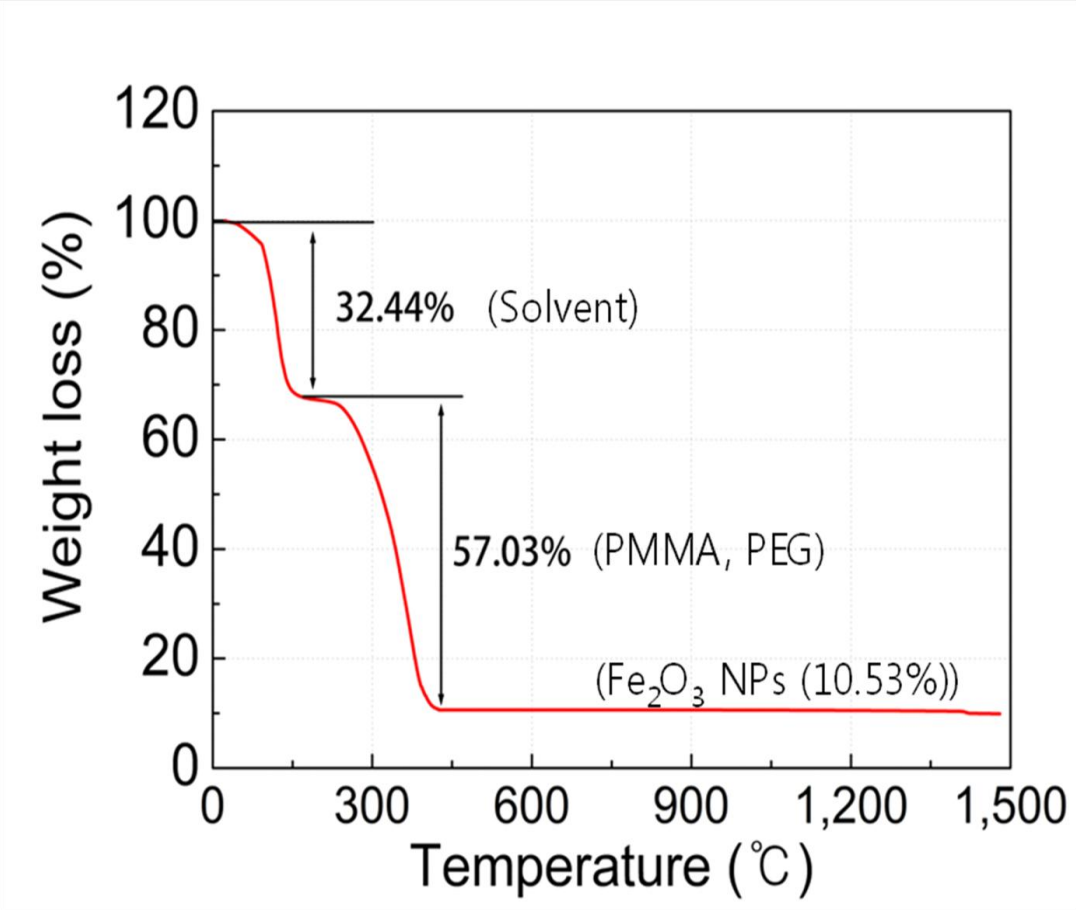

Figure 1. TGA was performed in an alumina pan and heated from room temperature to 1,500 °C at 25°C/min heating rate in air ambient to determine the materials decomposition and other changes on producing porous metal structure.

Figure 2 shows the influence of the ratio of Fe_2O_3 NPs to total amount of PMMA beads and PEG binder. At first, the composite layer is made with the composition of 0.12/1.00 (Fe_2O_3 NPs/total amount of PMMA and PEG) as shown in Figure 2(a). The amount of Fe_2O_3 NPs was doubled resulting in a composite layer with a ratio of 0.24/1.00 (Fe_2O_3 NPs/total amount of PMMA and PEG) as shown in Figure 2(b). Figure 2(b) indicates that the composite solution with too many Fe_2O_3 NPs fails to make adequate pores in the composite layer because the relative amount of PMMA beads is too small. With an increased amount of Fe_2O_3 NPs in the composite layer, the NPs tend to agglomerate and prevent a formation of a uniform porous metal structure. When a large amount of Fe_2O_3 NPs are used, it is difficult to mix the composite

uniformly which results in weak connections between Fe_2O_3 NPs. As seen in Figure 2(a), more porous structure can be fabricated with the composition of 0.12/1.00 (Fe_2O_3 NPs / total amount of PMMA and PEG) after burning process at 950°C for 2h. Both micro pores (15-20 um size) and the nano pores (100-500 nm size) are made in a somewhat uniform manner with this composite composition (0.12/1.00) and the porosity of this structure is expected to be higher than the structure with a larger amount of NPs as seen in Figure 2(b). The iron oxide structure of Figure 2(b) does not have micro-sized pores, but only nano-sized pores (100-500 nm) formed between Fe_2O_3 NP regions. The grain size in Figure 2(b) is similar to that of Figure 2(a) because of the same burning conditions utilized. The grain size in Figure 2(a) is about 1-2 um in average diameter.

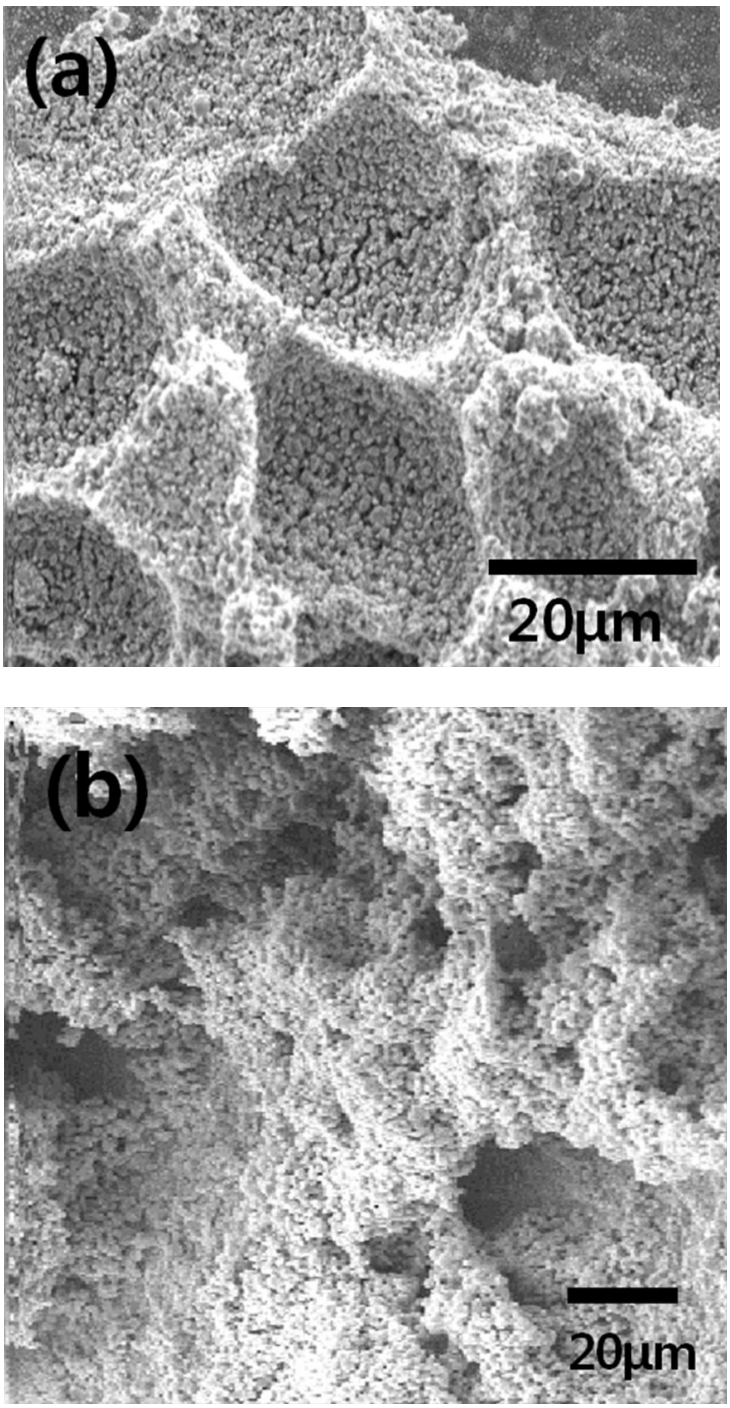

Figure 2. Representative SEM micrographs of porous structure having the Fe_2O_3 NPs ratio with PMMA beads + PEG solution (Sample was progressed burning process at 950°C for 2h in air). (a) Fe_2O_3 NPs : total amount of PMMA and PEG = 0.12 : 1.00, (b) Fe_2O_3 NPs : total amount of PMMA and PEG = 0.24 : 1.00.

The effect of increasing the PEG binder resin ratio was also studied, with the higher resin amount causing microcracking and damage to the uniform porous surface, which is visible in the SEM images compared in Figure 3. The PEG ratio is defined as the ratio of PEG to the total amount of Fe_2O_3 NPs and PMMA beads. When the structure is a composite with a PEG to NPs and PMMA ratio of 0.9/1.0 (PEG/total amount of Fe_2O_3 and PMMA), the burning process yields a structure that shows both nano-pores and distinct micro-pores that are uniformly distributed throughout the composite material as shown in Figure 3(a). In comparison, the composite solution with higher PEG ratio of 1.8/1 breaks the connection between micro-pores, which is likely a result of burning-out of the much larger agglomerated PEG resin located at interspace between micro-pores. This causes the formation of large cracks in the space between the micro-pores which the SEM image in Figure 3(b) exhibits. The porous iron oxide structure fabricated with PEG ratio of 0.9/1.0 contains micro-pores of 15-20 μm as well as nano-pores of 100-500 nm occupied between nano-grains, after the burning process at 950^{o}C for 2h in air atmosphere.

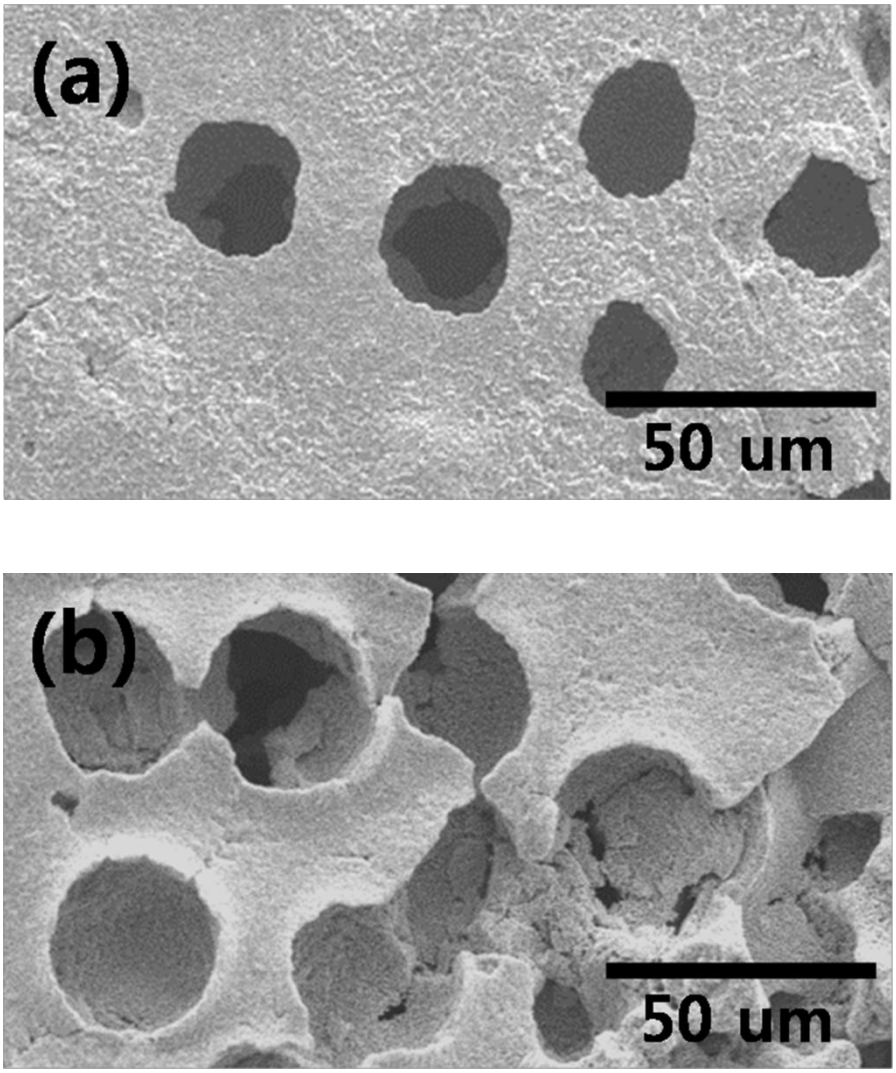

Figure 3. Representative SEM micrographs of porous structure according to PEG solution ratio with Fe_2O_3 NPs and PMMA beads (Sample was progressed burning process at 950 ℃ for 2 h in air not reduction) : (a) lower PEG binder ratio (PEG:total amount of Fe_2O_3 NPs and PMMA = 0.9:1.0) (b) higher PEG binder solution ratio (PEG:total amount of Fe_2O_3 NPs and PMMA = 1.8:1.0).

Figure 4 shows the influence of the burning temperature to the structure of the composite material. In the case of the burning process at 950°C for 2h, there are fewer connections between Fe_2O_3 NPs as seen in Figure 4(a). The burning at 950^{o}C is not high enough temperature to introduce satisfactory sintering of Fe_2O_3 NPs, by which the weaker connections are built in the porous structure of the type shown in Figure 4(a). To form a strong connection between Fe_2O_3 NPs, a higher sintering temperature is

needed. In the case of burning process at a higher temperature of 1,050°C, a strong connection between Fe_2O_3 NPs is made by a sufficient sintering as shown in Figure 4(b). However, the higher temperature 1,050°C can also decrease the amount of nano-pores compared to the burning at 950°C due to the coarsening. The porous iron oxide structure after burning at 1,050°C consists of larger grains of 2-3 μm size, compared to the grain size of 1-2 μm generated by 950°C annealing. Even though the porosity is expected to decrease a little, higher temperature burning at 1,050°C is more favorable for stronger and lighter structures.

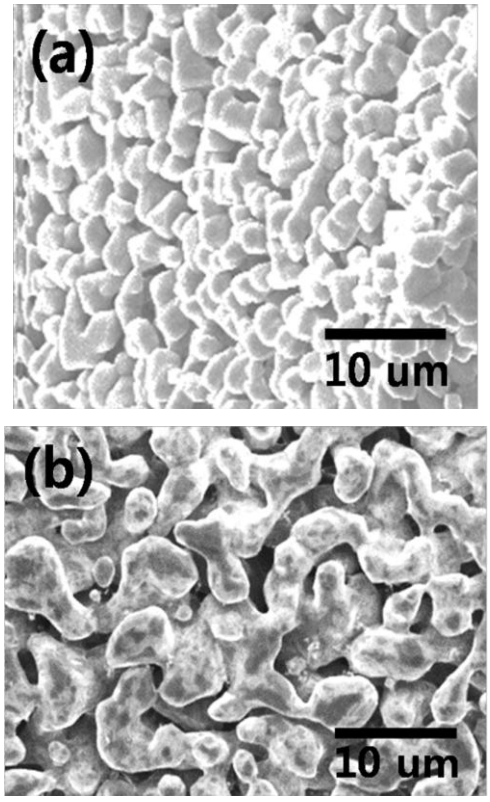

Figure 4. Representative SEM micrographs of porous structure after sintering at (a) 950°C and (b) 1,050°C for 2h in air at the same ratio (Fe_2O_3 NPs : total amount of PMMA and PEG = 0.12 : 1.00 (optimized condition based on Figure. 2 and Figure. 3 tests).

The reduction temperature can influence the porous iron structure as can be observed in Figure 5. Reduction process at 750°C for 5h in forming gas forms stronger connection of Fe network between micro-pores, as displayed in Figure 5(a). Even

though the porous iron structure fabricated with the reduction at 750°C has similar micro-pores (15-20 μm) to the porous iron structure formed with the reduction at 500°C (Figure 5(b)), the higher temperature reduction at 750°C can build stronger connection between Fe NPs judging from the SEM images. The inset images of Figure 5 are showing the internal structures of reduced samples. Too many nano-pores between iron NPs formed by reduction at 500°C for 5h makes Fe network to be weaker, which is attributed to the smaller total area of good bonding between Fe NPs.

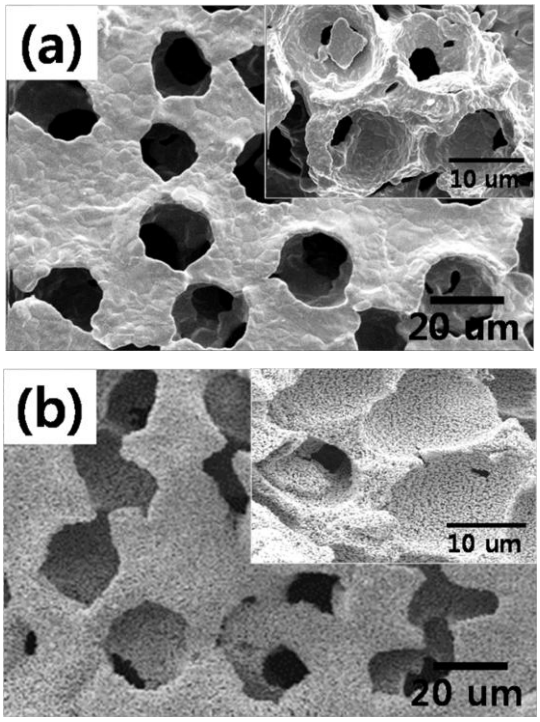

Figure 5. Representative SEM micrographs of porous structure according to heat treatment –reduction temperature after burning process at 1050°C for 2h in air: (a) Surface and internal configuration of the porous metal structure reduced at 750°C for 5h in forming gas; (b) Surface and internal configuration of porous metal structure reduced at 500°C for 5h in forming gas at the same ratio (Fe_2O_3 NPs : total amount of PMMA and PEG=0.12 : 1.00 (optimized condition based on Figure. 2 and Figure. 3 tests).

Figure 5(c) ~ (f) show EDX and XRD results vs the reduction temperature in forming gas atmosphere. When this reduction is carried out at 500°C for 5h in forming gas, the iron oxide phase in a porous structure is not completely reduced to iron phase based on the analysis EDX and XRD as can be seen from Figure 5(d) and Figure 5(f).

The EDX analysis detects oxygen at 0.5 keV in Figure 5(d). But there is no oxygen peak detected in Figure 5(a) obtained by the reduction at 750°C, which means iron oxide is transformed into pure iron in porous structure. The XRD data in Figure 5(e) indicates that iron oxide (Fe_2O_3) existing in porous structure after polymer/binder burning-out can be reduced completely into pure Fe which has a main plane of (102) in primitive hexagonal crystal structure when Fe_2O_3 is annealed at 750°C for 5h in forming gas. But the temperature of 500°C is not high enough to reduce all Fe_2O_3 to pure Fe, because Figure 5(f) exhibits the mixed crystal structures of Fe (body-centered cubic structure),[16] Fe_3O_4 (face-centered cubic structure)[17] and Fe_2O_3 (rhomb-centered rhombohedral structure). [18] Based on the results of EDX and XRD analysis, the reduction condition can be optimized to be 750°C / 5h under a forming gas.

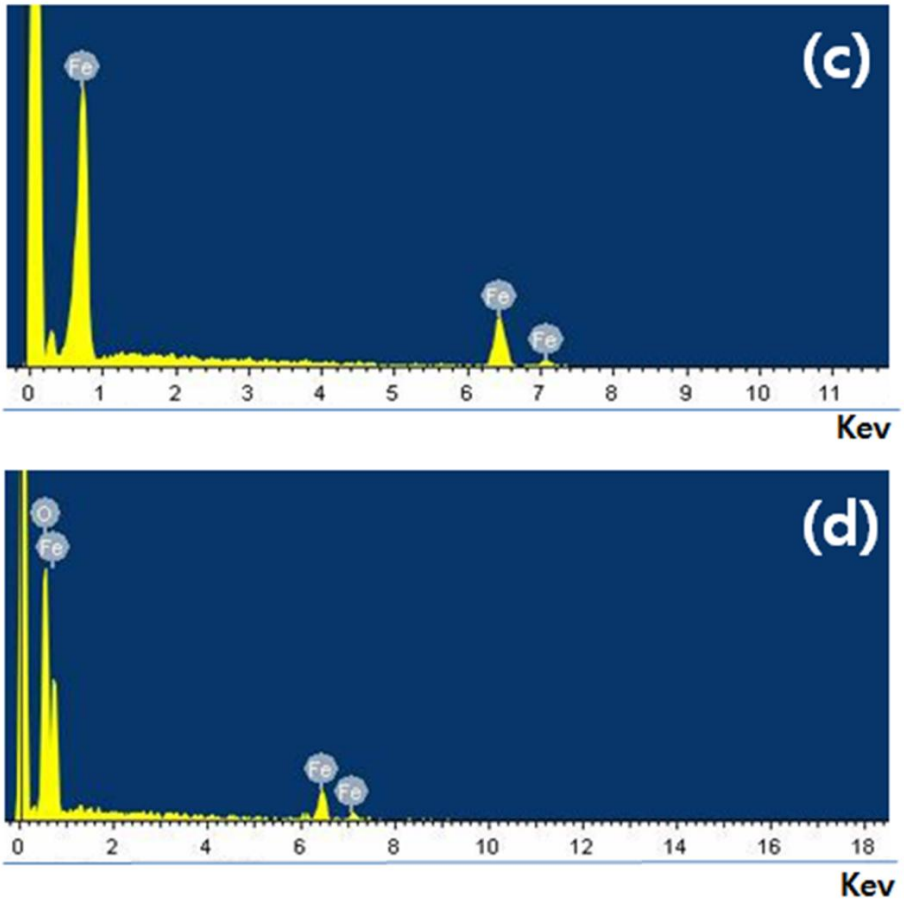

Figure 5. EDX spectra of porous structure according after reduction at (c) 750°C and (d) 500°C for 5h in forming gas (H_2:N_2 = 5:95), Continued.

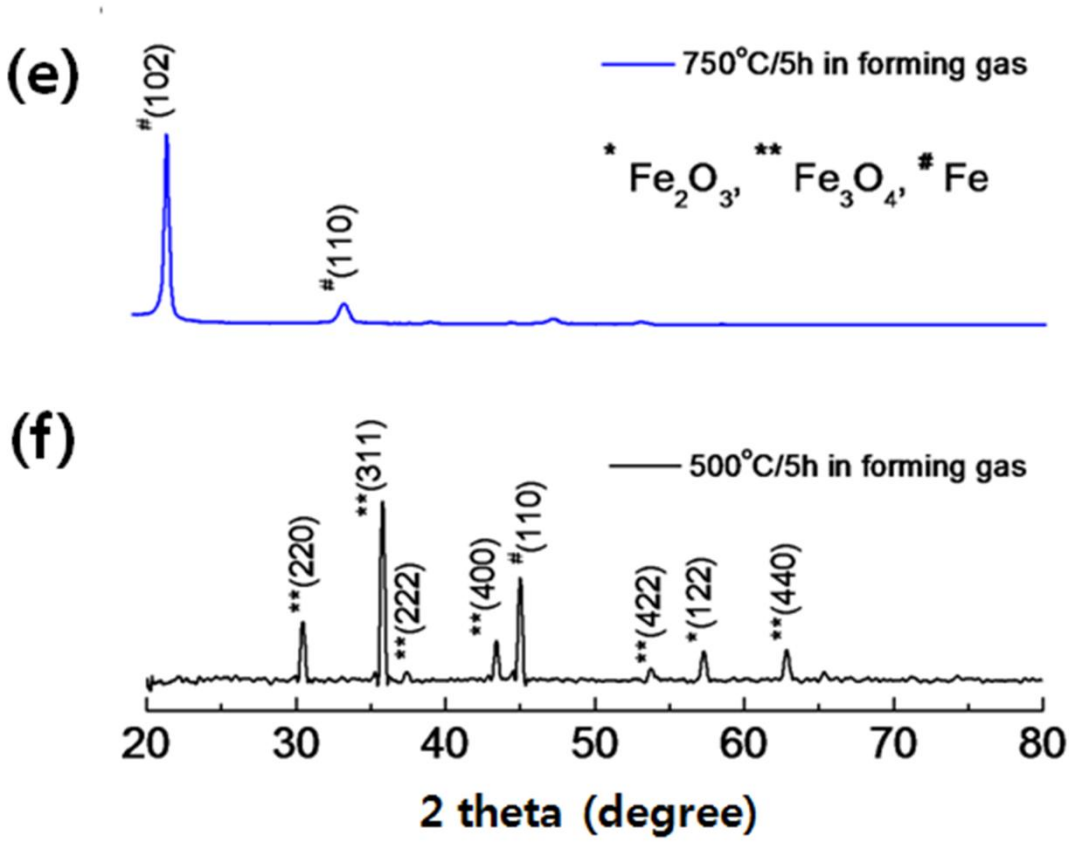

Figure 5. XRD analysis showing the crystal structures obtained by the reduction at (e) 750°C/5h, and (f) 500°C/5h in forming gas. (H_2:N_2 = 5:95), Continued.

To optimize the procedure for the porous iron structure, the various conditions and their results which were explained in the previous paragraphs are summarized in Table 1. The optimized composite slurry is composed of Fe_2O_3 with a ratio of 0.12/1.0 (Fe_2O_3/total amount of PMMA and PEG) and PEG with a ratio of 0.9/1.0 (PEG/total amount of Fe_2O_3 and PMMA). The proper heat-treatment conditions include the burning process at 1050°C for 2h in air followed by the reduction procedure at 750°C for 5h in forming gas.

Table 1. Optimum conditions needed to produce a porous metal structure based on Fe.

Fig No.	Fe_2O_3* or PEG**	Burning	Reduction	Pore size		Porosity	Grain Size (μm)	Network Connection
				Micro Pore (μm)	Nano Pore (nm)			
2(a)	(Fe_2O_3*) 0.12 : 1[a]	950℃ 2 h /air	**X**	15~20	100~ 500	High	1 ~ 2	Bad
2(b)	(Fe_2O_3*) 0.24 : 1[a]	950℃ 2 h/air	**X**	0 ~5	100 ~ 500	Low	1 ~ 2	Bad
3(a)	(PEG**) 0.9 : 1[b]	950℃ 2 h/air	**X**	15~ 20	100 ~ 500	High	1 ~ 2	Many cracks
3(b)	(PEG**) 1.8 : 1[b]	950℃ 2h/air	**X**	15~ 20	100 ~ 500	High	1 ~ 2	No crack
4(a)	(Fe_2O_3*) 0.12: 1[c]	950℃ 2 h/air	**X**	15~ 20	100 ~ 500	High	1 ~ 2	Bad
4(b)	(Fe_2O_3*) 0.12: 1[c]	1,050° C 2 h/air	**x**	15~ 20	100 ~ 500	High	2 ~ 3	Good
5(a)	(Fe_2O_3*) 0.12: 1[c]	1,050° C 2 h/air	750℃/5h forming gas	15 ~20	100 ~ 500	Low	2 ~ 3	Good
5(b)	(Fe_2O_3*) 0.12: 1[c]	1,050° C 2 h/air	500℃/5h forming gas	15~ 20	100 ~ 500	High	2 ~ 3	Bad

* The ratio of Fe_2O_3 to total amount of PMMA and PEG.
** The ratio of PEG to total amount of PMMA and Fe_2O_3.
[a] (PMMA : PEG = 0.2 : 0.8)
[b] (Fe_2O_3 : PMMA = 0.36 : 0.64)
[c] (PMMA : PEG = 0.47 : 0.53)

2.3 Conclusions

Introducing a nano-structure by altering conventional materials structure leads to the development of light-weight and stronger materials, which is important for many industrial applications. In this research, we investigated the desired process conditions to produce a porous metal structure of iron. The optimization of the composition and procedures were made by focusing on different mix ratio compositions related to proper ratio of Fe_2O_3 NPs, PEG binder, and PMMA beads and studying the heat treatment procedure which is critical for formation of nano-pore structure. In this study, the optimized composite slurry is composed of Fe_2O_3 with a ratio of 0.12/1.00 (Fe_2O_3/total amount of PMMA and PEG) and PEG with a ratio of 0.9/1.0 (PEG/total amount of Fe_2O_3 and PMMA). The optimal heat-treatment condition was found to include the burning process at 1050^{o}C for 2h in air followed by the reduction procedure at 750^{o}C for 5h in a forming gas.

CHAPTER 3: Overall Summary, Conclusions, and Future Work

Porous metal structure has applications in many fields including the light-weight transportation structures such as automobiles, trains and airplanes as well as the defense industry for military helmets or assault jackets to allow for more protection to the soldiers.

REFERENCES

1. Dybtsev DN, Chun H, Kim K. Rigid and Flexible : A highly porous metal–organic framework with unusual guest–dependent dynamic behavior. Angew. Chem. 2004 ; 116 : 5143-5146.

2. Banhart J, Leyda B. Aluminum foams : On the road to real applications. MRS Bulletin. 2003 April ; 28 : 290-295.

3. Jiang HL, Xu Q. Porous metal-organic frameworks as platforms for functional applications. Chem Comn. 2011 ; 47 : 3351-3370.

4. Shen YF, Lu L, Lu QH, Z, Jin ZH, Lu K. Tensile properties of copper with nano-scale twins. Scripta Mater. 2005 ; 52 : 989-994.

5. Ryan G, Pandit A, Apatsidis DP. Fabrication methods of porous metals for use in orthopaedic applications. Biomaterials. 2006 ; 27 : 2656-2670.

6. Winnett J, Mallick KK. Parametric characterization of porous 3D bioscaffolds fabricated by an adaptive foam reticulation technique. JOM. 2014 ; 66 : 591-597.

7. Badwal SPS, Rajendran S. Effect of micro-and nano-structures on the properties of ionic conductors. Solid State Ionics. 1994 ; 70 : 84-95.

8. Li WL, Tao NR, Lu K. Fabrication of a gradient nano-micro-structured surface layer on bulk copper by means of a surface mechanical grinding treatment. Scripta Mater. 2008 ; 59 : 546-549.

9. Zaluska A, Zaluski L, Ström-Olsen JO. Structure, catalysis and atomic reactions on the nano-scale : a systematic approach to metal hydrides for hydrogen storage. Applied Physics A. 2001 ; 72 : 157-165.

10. Grässel O, Krüger L, Frommeyer G, Meyer LW. High strength Fe±Mn±(Al, Si) TRIP/TWIP steels development Ð properties Ð application. Int. J. Plast. 2000 ; 16 : 1391-1409.

11. Townsend TK, Sabio EM, Browning ND, Osterloh FE. Photocatalytic water oxidation with suspended alpha-Fe_2O_3 particles-effects of nanoscaling. J. R. Soc. Chem. Perkin. 2011 ; 4 : 4270-4275.

12. Apte S, Yang V. Unsteady flow evolution in porous chamber with surface mass injection, part 1: free oscillation. AIAA JOURNAL. 2001 August ; 39 : 1577-1586.

13. Mercier L, Pinnavaia TJ. Access in mesoporous materials : advantages of a uniform pore structure in the design of a heavy metal ion adsorbent for environmental remediation. Advanced Materials. 1997 ; 9 : 500-503.

14. Dresselhaus MS, Thomas L. Alternative energy technologies. Nature. 2001; 414 : 332-337.

15. Davis ME. Ordered porous materials for emerging applications. Nature. 2002 ; 417 : 813-821.

16. Owen EA, Williams GI. A low-temperature X-ray camera. J. Sci. Instrum. 1954 ; 31 : 49-54.

17. Sasaki S. Radial distribution of electron density in magnetite, Fe_3O_4. Acta Cryst. 1997 ; 53 : 762-766.

18. Sawada H. An electron density residual study of a-ferric oxide. Mater. Res. Bull. 1996 ; 31 : 141-146.